Engineering Structures 300 (2024) 117203

Contents lists available at ScienceDirect

Engineering Structures

journal homepage: www.elsevier.com/locate/engstruct

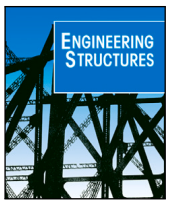

Seismic experimental analysis of a full-scale steel building with passive fire protections

Patrick Covi [a], Nicola Tondini [a,*], Marco Lamperti Tornaghi [b], Francisco-Javier Molina [b], Pierre Pegon [b], Georgios Tsionis [b]

[a] Department of Civil, Environmental and Mechanical Engineering, University of Trento, via Mesiano 77, Trento, 38123, Italy
[b] Joint Research Centre (JRC), Bld. 48, via Enrico Fermi 2749, 21027 Ispra, Italy

ARTICLE INFO

Keywords:
Concentrically braced steel frame
Earthquake
Experimental tests
Fire
Fire following earthquake
Fire protection
Hybrid simulation
Seismic
Steel

ABSTRACT

The paper describes the results of an experimental campaign on the seismic behaviour of a full-scale concentrically braced steel frame designed according the EC8 and equipped with different types of passive fire protection. In this respect, fire protection boards made of calcium silicate and mineral spray-based fire protections were applied to dissipative members, such as the bracings, and to non-dissipative elements, such as one column of the bracing system. Two solutions of calcium silicate fire protection boards were employed: (i) a standard solution and (b) an improved solution conceived for seismic applications. Moreover, the external bays of the specimen equipped with mineral spray-based fire protections were filled with two fire walls both of them made of concrete blocks without and with seismic detailing, respectively. In total 10 tests on 4 frames, that also include a first test of the bare frame, were performed, and for each test different seismicity levels were applied. The hybrid simulation technique was used to maintain the relevance and accuracy of a full-scale test and also to optimize the use of the available test facilities. In this respect, only the ground floor of the prototype structure was physically tested in the laboratory, whereas the remainder of structure was numerically simulated. The tests showed that the fire protections and the fire walls did not suffer major damage owing to cyclic loading. Indeed, the damage was not likely to significantly affect the fire performance. The outcomes of the experimental results of all the tests are thoroughly described in the paper.

1. Introduction

1.1. Background and motivation

Earthquakes are destructive and unpredictable events with catastrophic consequences for both people and built environment [1,2]. Moreover, secondary triggered effects can strike further an already weakened community, i.e. landslides and tsunamis. In this respect, also fires following earthquake (FFE) have historically produced large post-earthquake damage and losses in terms of lives, buildings and economic costs, like the San Francisco earthquake (1906), the Kobe earthquake (1995), the Turkey earthquake (1999), the Tohoku earthquake (2011) and the Christchurch earthquakes (2011). In detail, FFE pose a considerable potential threat as they can be widespread both at the building level and at the regional level within the seismic affected area [3] owing to the rupture of gas lines, failure of electrical systems etc. [4] and at the same time failure of the fire compartmentation measures and because fire brigades should be also engaged in rescue operation after earthquake. Moreover, they are more difficult to tackle by the fire brigades because of their possible large number and extent, as well as of possible disruptions within the infrastructural network that hinder their timely intervention and within the water supply system [5,6].

In this context, the structural fire performance can worsen significantly because the fire acts on an already damaged structure [7]. Furthermore, passive and active fire protections may have also been damaged by the seismic action and the fire can spread quickly if compartmentation measures have failed [8]. Thus, the seismic performance of the non-structural components may directly affect the fire performance of the structural members. Consequently, minimization of the non-structural damage is paramount in mitigating the possible drop in structural fire performance. The loss of fire protection is particularly dangerous for steel structures because the high thermal conductivity associated with small profile thicknesses entails quick temperature

* Corresponding author.
E-mail address: nicola.tondini@unitn.it (N. Tondini).

https://doi.org/10.1016/j.engstruct.2023.117203
Received 2 March 2023; Received in revised form 24 October 2023; Accepted 19 November 2023

rise with consequent fast degradation of strength and stiffness [9,10]. Moreover, the post-fire assessment of the steel members becomes significant [11]. Experimental research at the element or component level was performed.

In greater detail, a series of quasi-static cycling tests on the seismic performance of sprayed fire-resistive material applied to the steel elements were carried out by Braxtan et al. [12]. Damage to the fireproofing was observed after the tests. The same research group [13] later investigated the post-earthquake fire performance of a steel moment-resisting frame protected with sprayed fire-resistive material. Pucinotti et al. [14,15] experimentally analysed the post-earthquake fire behaviour of beam-to-concrete filled steel tube column joints. Steel–concrete composite beam-to-column joints partially damaged by cyclic loading were investigated at elevated temperatures by Ye et al. [16]. Moreover, Song et al. [17] investigated the fire behaviour of unstiffened welded steel I-beam to hollow column connections subjected to the post-earthquake scenario. The results showed that severe damage would significantly affect the performance of the connections under post-earthquake fire. Imani et al. [18] performed an experimental campaign on concrete-filled double-skin tube columns subjected to fire after two different simulated seismic loads and using a specific boundary condition (fixed and semi-fixed ends). The comparison results between the two damaged columns and the undamaged column showed that the seismic damage level had insignificant effects on the fire resistance time of the specimens. Wang et al. [19] studied the residual capacity and mechanical behaviour of circular concrete-filled steel tubular columns exposed to the post-earthquake fire. The experimental results indicate that these types of columns generally performed well after a fire following earthquake event. Lou et al. [20] investigated the structural response and failure procedure of a self-centring steel system subjected to fire following earthquake.

Regarding experimental research on large-scale specimens, a full-scale test on a reinforced concrete frame was performed by Kamath et al. [21] to investigate the fire response after a seismic event. A large-scale test was carried out at the University of California, San Diego (UCSD), to study the post-earthquake performance of a 5-storey reinforced concrete building [22,23]. The seismic damage was induced by means of the shaking table, and tests with seismic isolation and fixed-base were performed. Fire tests were then carried out to analyse the performance of non-structural components. Shah et al. [24] presented the outcomes of a full-scale on seismically damaged RC frames subjected to post-earthquake fire. The results showed that seismic damage affected the rise in temperatures in the structural elements. The experimental research conducted by Hutchinson et al. [25] summarizes the global responses, the physical damage, the shear wall behaviour protected with 16-mm thick gypsum boards, and the design implications of a full-scale 6-storey cold-formed steel-framed building test campaign that involved earthquake and live fire testing at two select floors.

Tests on non-structural components were performed by Calayir et al. [26] that investigated the performance of fire door sets after experiencing simulated earthquake damage. The earthquake effects were imposed using a quasi-static cyclic loading test procedure. The results of cyclic load tests showed severe distortion of the fire door frames and excessive gaps, while results of the subsequent post-earthquake fire test showed a decrease of the fire resistance up to 70%. The experimental research conducted by Tian et al. [27] presents the results of an experimental program designed to evaluate the seismic behaviour of fire extinguishing sprinkler piping systems. Three full-scale specimens spanning two-floor levels were tested with three different pipe materials and various bracing configurations. The results showed some damage to the sprinkler heads, failures of vertical hangers, and a complete branch line fracture. Moreover, useful information on the seismic damage to relevant non-structural components that can affect the fire development, such as glazing, partition walls, and doors, are presented and quantified using fragility functions in Federal Emergency Management Agency P58 background documentation [28].

Shaking table testing is an effective experimental method to understand the dynamic behaviour of a structure, while hybrid simulation (HS), also known as pseudodynamic technique [29], allows a better focus on the interaction between structure and substructure [30]. Indeed, several research works have been conducted in the past, e.g. on a reinforced concrete viaduct where two piers were physically tested, whereas the other piers and the deck were numerically simulated [31]; HS tests of a steel frames equipped with easily replaceable dissipative elements for which the ground floor was physically tested and the upper floors constituted the numerical remainder of the structure, were performed [32,33]. Moreover, Memari et al. [34] carried out a hybrid simulation test on a small-scale steel-braced frame under fire and FFE.

The issue of post-earthquake fire performance of protected structural systems has not received much attention despite its importance. This research aims to fill this gap by presenting new experimental data from full-scale tests, also using a hybrid simulation technique to account for the boundary conditions of the specimen, which represents a full-scale part of a larger building.

The literature analysis also reveals that few studies on the experimental behaviour of the interaction between structural and fire-resistant non-structural components were performed. Therefore, this research, funded within the European Transnational Access project EQUFIRE, aims to provide more experimental data on the behaviour of passive fire protections made of silicate calcium boards and spray-based vermiculite applied to the structural members composing a steel-braced frame subjected to seismic loading. In particular, since no provisions exist for seismic areas, both standard fire protection boards and seismically improved boards were tested by means of the hybrid simulation technique. Moreover, according to the capacity design philosophy both the dissipative members, i.e. the bracings and the non-dissipative member, i.e. the columns of the bracing system, were equipped with passive fire protections. The paper is organized as follows: In Section 2, the design of the prototype structure is presented; in Section 3, the ground motion selection is described, whilst Section 4 reports on the numerical model and the preliminary simulations targeted to the tests; Section 5 presents the experimental campaign; Section 6 describes the test outcomes and finally, in Section 7 the conclusions along with the future perspectives are drawn.

2. Design of the prototype building

A four-storey, three-bay steel building with concentric bracings in the central bay was selected as a case study, as shown in Fig. 1. It was located in Lisbon, Portugal, in an area of medium seismicity. Since the experimental tests were conducted on full-scale specimens, the design of the structure was influenced by the laboratory capacity in terms of maximum available dimensions, applied force and displacement. In particular, it is an office building with a square plan (12.5 m × 12.5 m), as reported in Fig. 2. The storey height is 3 m, except the first floor, which is 3.6 m high. The selection of 3.6 m was due to the furnace height at BAM, where FFE tests on columns were made [35]. The lateral-resisting system is made of I-profile sections with the weak axis oriented in the plane of the frames to force in-plane buckling. This choice was essentially made for two reasons: (i) to avoid possible damage in the walls where the bracing is inserted owing to out-of-plane buckling; (ii) to keep a 2D modelling of the frame meaningful and consequently to reduce the computational demand for the hybrid simulation, because the tests and the simulations were performed on bi-dimensional frames. Two different steel grades were used, namely S275 and S355. S275 was employed for the dissipative elements, i.e. the bracing system, while S355 was selected for the non-dissipative members, i.e. columns and beams. The loads on the frame selected for the test and the type of profiles are shown in Fig. 3. The composite floor is formed of a steel I-section, which is connected to a concrete

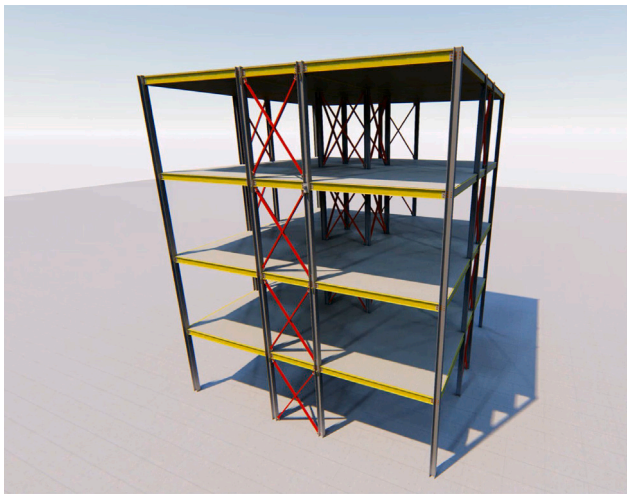

Fig. 1. EQUFIRE case study: Isometric view of the structure.

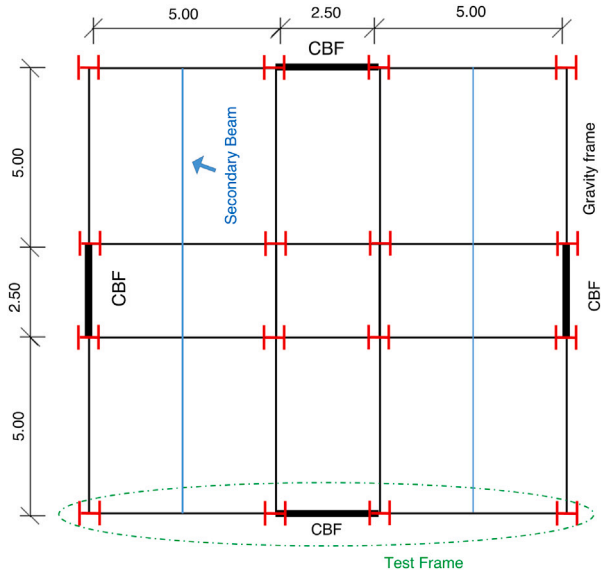

Fig. 2. Typical floor framing plan. Dimensions in m.

slab with a 1 mm thick cold-formed profiled steel sheeting element perpendicular to the beam with a mesh reinforcement of diameter 6-mm spaced at 100-mm spacing. The height of the ribs is 55 mm and the total height of the slab is 120 mm (see Fig. 4). In this way, it could be considered as a rigid diaphragm that simplified the seismic analyses. The concrete strength class was C30/37. Moreover, the composite solution prevents lateral–torsional buckling, and this allows keeping meaningful 2D modelling.

The structural weight of the slab is equal to 2.0 kN/m^2. The non-structural weight of a typical floor and of the roof are respectively 2.7 kN/m^2, and 1.3 kN/m^2. The weight of the curtain wall is estimated as 8.44 kN/m^2. The value of the imposed load for an office occupancy is specified as 2.0 kN/m^2 according to EN 1991-1-1 [36], while for the roof, a value of 0.5 kN/m^2 for the snow load was considered. The latter was computed according to EN 1991-1-3 [37] by considering that the building was located at 2 m above sea level and that there was no significant snow removal by wind in the building area. So, the normal topography ($C_E = 1$) value coefficient was adopted.

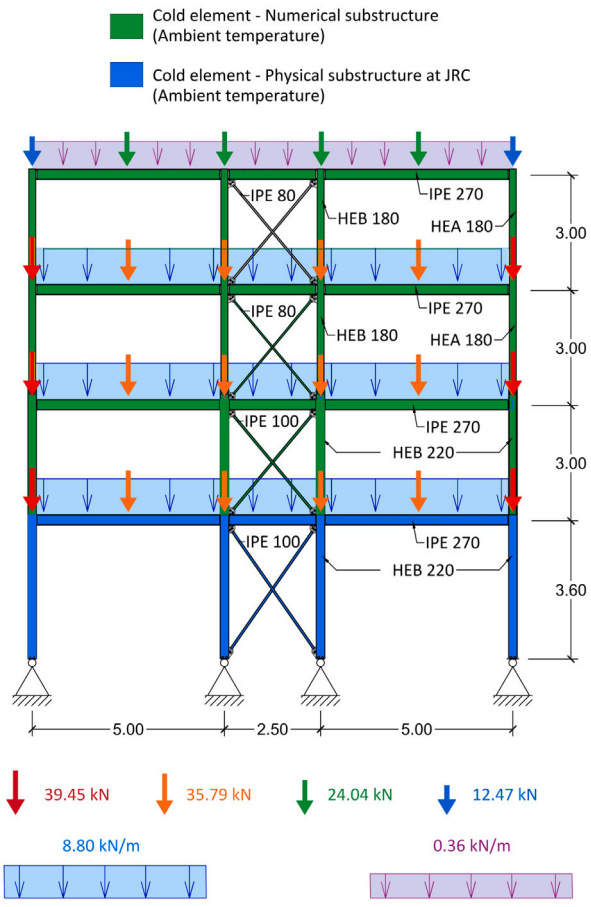

Fig. 3. Frame geometry and loads. Dimensions in m.

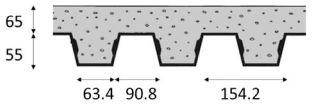

Fig. 4. Section of cold formed profiled steel sheeting element. Dimensions in mm.

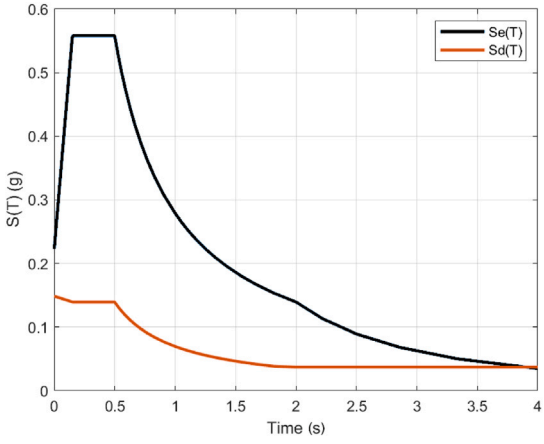

Fig. 5. Elastic spectrum $S_e(T)$ and design spectrum $S_d(T)$.

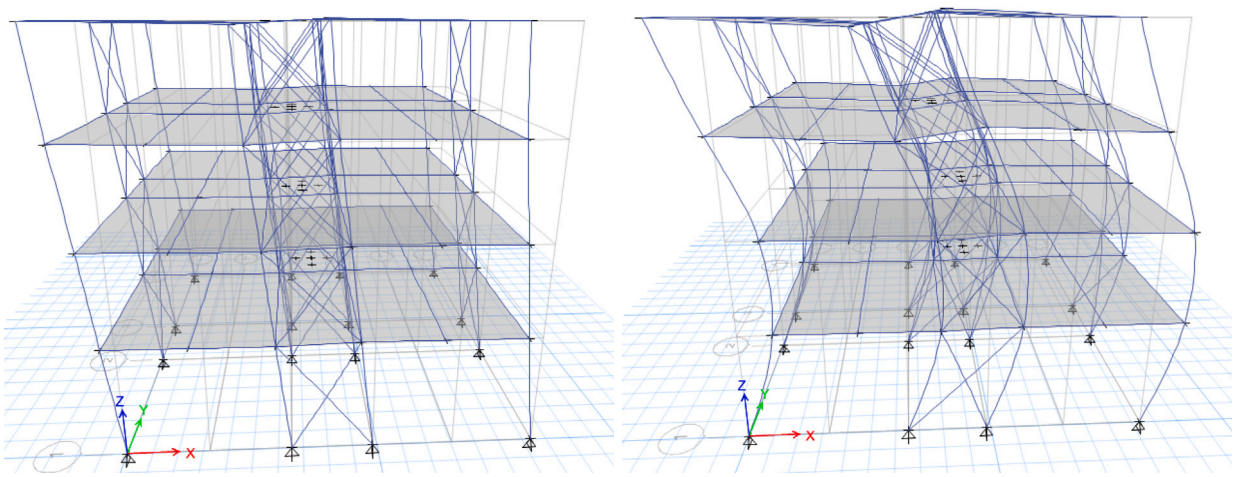

Fig. 6. Translational modes along UX: (a) Mode 1 and (b) Mode 4.

2.1. Seismic design

The design of the lateral-resisting system of the building was governed by the seismic action. In accordance with EN 1998-1 [38], the frame was seismically designed according to the capacity design criterion, which means that dissipation is expected in the bracing members. A high ductility class (DCH) was selected, entailing a behaviour factor equal to 4 for regular elevation systems. The seismic design was performed in accordance with EN 1998-1 [38] and the forces and displacements were obtained by means of a linear 3D dynamic analysis with response spectrum. A Significant Damage limit state, i.e. life safety limit state, only the diagonal in tension of the bracing system was modelled. The columns were considered continuous along the height of the structure and all connections of the beams and diagonals were assumed as pinned. Given the slab thickness of 6.5 cm, the rigid diaphragm condition was applied and masses were lumped at the floors. In terms of regularity, the building is both regular in plan and in elevation. Moreover, it is located on a type B soil and a seismic importance factor equal to 1 was assumed.

For the seismic part, a general design described by the EN 1998-1 [38] was adopted without using national annexes. The only exception was for the determination of the reference peak ground acceleration. Indeed, based on the study of Silva et al. [39], the building was located in an area where the reference peak ground acceleration equals a_g = 0.186 g and type B soil. The seismic action type 1, characterized by long-distance severe magnitude earthquakes for a 475-year return period (Life safety limit state), was selected. The lower bound factor β for the design response spectrum was assumed to equal 0.2 [38]. As a result, the elastic and the design spectra are shown in Fig. 5. The parameters of the elastic response spectrum are reported in Table 2.

To perform the linear dynamic analysis with the response spectrum, a 3D model of the prototype structure was developed in OpenSees [40]. The first nine modes were considered based on the modal masses, as shown in Table 1. The two first translational modes along the direction of testing are shown in Fig. 6.

Table 1
Periods of the structure and modal masses.

Mode	Dir.	T (s)	m_x (%)	m_y (%)	m_z (%)
1	UX	0.674	83.9	0	0
2	UY	0.674	0	83.3	0
3	RZ	0.682	0	0	84.4
4	UX	0.223	14.3	0	0
5	UY	0.223	0	14.1	0
6	RZ	0.208	0	0	13.8
7	UX	0.123	1.3	0	0
8	UY	0.119	0	1.4	0
9	RZ	0.116	0	0	1.3

2.2. Fire design

The building was designed to withstand an exposure to the standard ISO 834 fire curve for 60 min in accordance with the fire requirements foreseen in Portugal for an office occupancy building of height 12.6 m and less than 1000 occupants. Since the unprotected structure was not capable of satisfying such requirement, two types of passive fire protection were envisaged, i.e. boards made of calcium silicate and mineral spray-based protection based on vermiculite and gypsum, whose properties are reported in Table 3 and are typical of protection materials that can be found on the market. The thickness of the protections was selected equal to 20 mm and this choice was also based on application purposes. Indeed, different applications were conceived:

1. Boards of calcium silicate with a standard application using staples were employed, as depicted in Fig. 7a.
2. Boards of calcium silicate designed to achieve better behaviour under seismic loading by adding a metallic substructure and using screws to connect the boards, as shown in Fig. 7b. The metallic substructure consists of steel angles (50 mm × 50 mm × 6 mm).
3. Spray-based protection with a plastic-coated galvanized metallic mesh for better adhesion in seismic regions of the spray-based protection, as illustrated in Fig. 7c. The mesh size is 2 in (51 mm) hexagonal and the wire diameter is equal to 1.5 mm.

The seismic performance of such fire protections was then assessed in the experimental campaign described in this work. Moreover, they were also tested in FFE tests at BAM, that it will be part of future works.

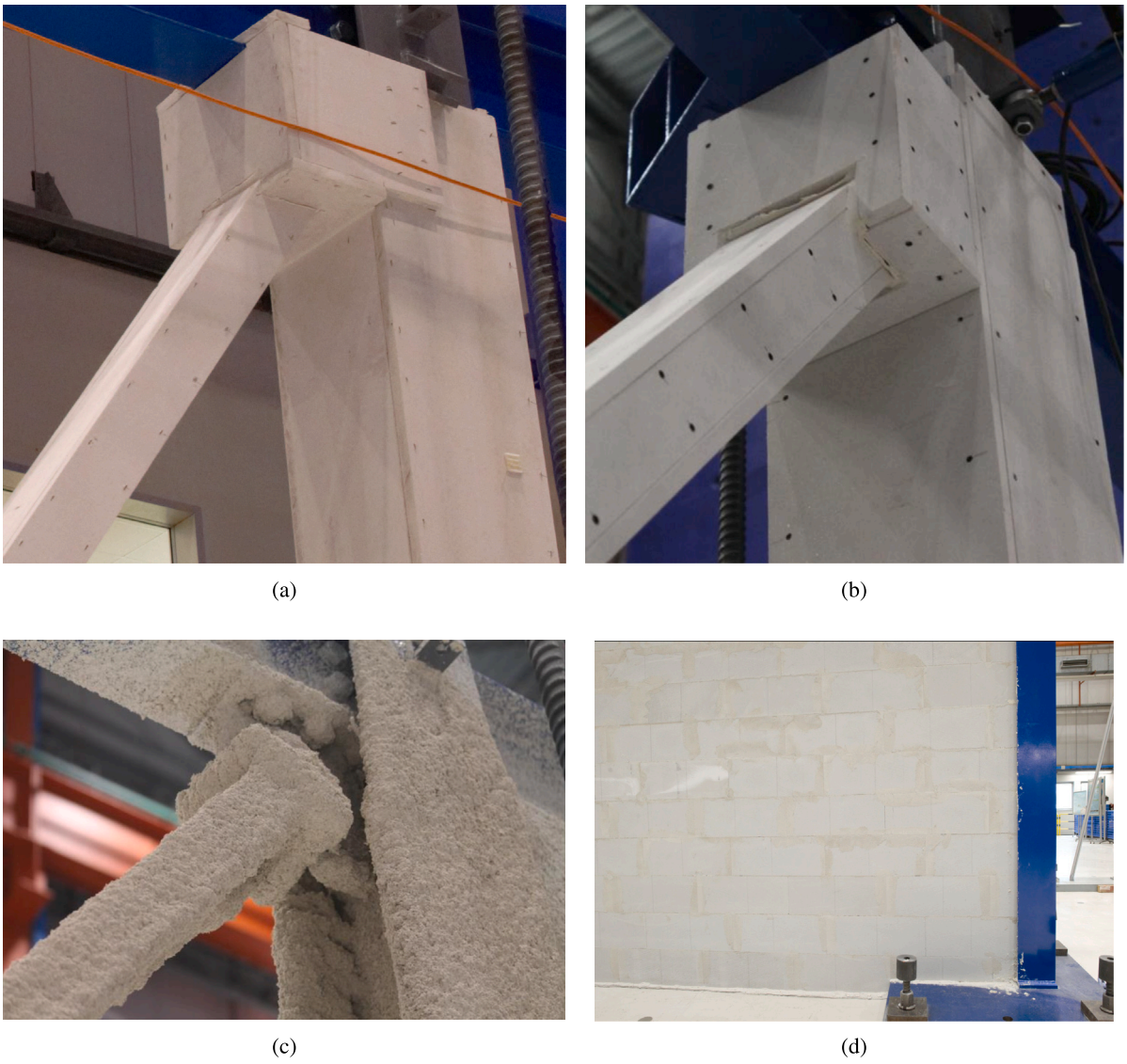

Fig. 7. Fire protections: (a) boards of calcium silicate with a standard application; (b) boards of calcium silicate for seismic region; (c) vermiculite spray-based protection; (d) firewall.

Table 2
Parameters of the elastic response spectrum.

Parameter	Description	Value
S	Soil factor	1.2
T_B	Lower limit of the period of the constant spectral acceleration branch	0.15 s
T_C	Upper limit of the period of the constant spectral acceleration branch	0.25 s
T_D	Value defining the beginning of the constant displacement response range of the spectrum	1.2 s

In addition to the fire protections applied to steel members, firewalls were also envisaged to subdivide the different compartments within the prototype building. They were also tested to verify whether they could provide effective fire compartmentation without altering the seismic response of the frame. In particular, the walls were made of autoclaved aerated concrete blocks of thickness 200 mm. Two different solutions were tested: (i) a firewall without any measure against the seismic action (Fig. 8a); (ii) a firewall with reinforcement that consisted of two parallel wires welded together with a continuous truss wire between the blocks (Fig. 8b). The aim was to increase the strength of the masonry and delay cracking.

3. Ground motion selection

As previously mentioned, the design of the prototype structure was affected by laboratory constraints inherently present at the JRC and at the BAM. This also applied to the ground motion selection. Indeed, the following constraints had to be considered when choosing the ground motion record to use in the experimental campaign:

- The selected accelerogram had to cause significant damage to the bracing elements.
- The horizontal displacement of the first floor had to be equal to or lower than ±30 mm to be compatible with the stroke of the

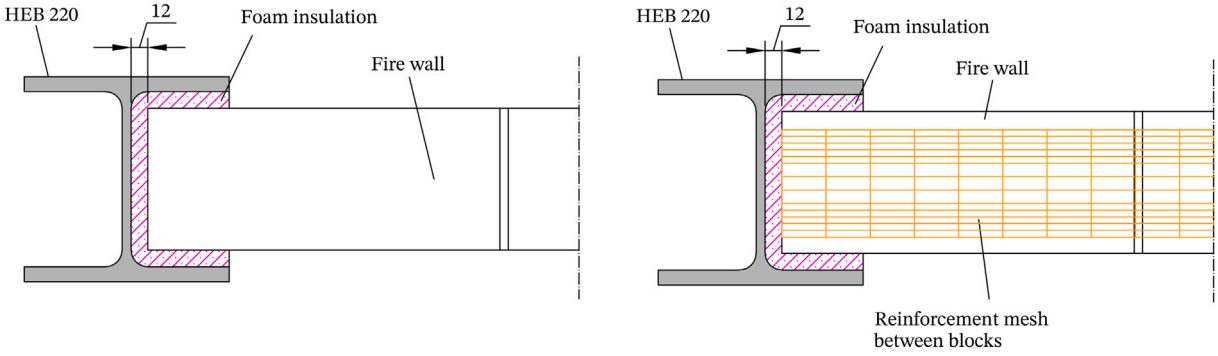

Fig. 8. Firewall connection details: (a) without seismic detailing; (b) with seismic detailing. Dimensions in mm.

Table 3
Technical data of the passive fire protections.

Boards made of calcium silicate	
Bulk density	870 kg/m^3
Thermal conductivity	0.17 W/m K (20 °C) 0.19 W/m K (100 °C) 0.21 W/m K (200 °C)
Specific heat capacity (400 °C)	0.92 kJ/kg K
Modulus of elasticity E Longitudinal/Lateral	4200/2900 MPa
Bending strength Longitudinal/Lateral	7.6/4.8 N/mm^2
Tensile strength Longitudinal/Lateral	4.8/2.6 N/mm^2
Compressive strength at ambient temperature	9.3 N/mm^2
Mineral spray-based protection based on vermiculite and gypsum	
Density (theoretical)	365 kg/m^3
Thermal conductivity	0.078 W/m K (20 °C)
Specific heat capacity	0.949 kJ/kg K

horizontal actuator inside the BAM furnace. This entailed a maximum inter-storey drift ratio of 0.8%, which is a value in between the life safety (1.5%) and immediate occupancy (0.5%) limit states for steel braced frames according to the FEMA-356 [41].

- The axial force of the interior columns at the base of the second floor had to be below 1000 kN to be compatible with the actuators used to impose the vertical loads on the specimen at the ELSA Reaction Wall.

On these premises, a set of fifteen accelerograms was selected considering the target spectrum, earthquake scenario (magnitude range, distance range, style-of-faulting), local site conditions, period range, and ground motion components using the INGV/EPOS/ORFEUS European strong motion database [42]. Among the fifteen accelerograms, the one shown in Fig. 9a was selected for the experimental hybrid simulation tests. The selected seismic action was represented by a natural accelerogram recorded during the Patras earthquake in 1994 with peak ground acceleration (PGA) equal to 0.2 g. It was then modified to be compatible with the Eurocode 8 (EN 1998-1 [38]) elastic response spectrum type B used in the seismic design (see Section 2) in the period range of 0.4 s–0.9 s, which includes the structure fundamental period, as shown in Fig. 9b. The parameters of the elastic spectrum are reported in Table 2. Its selection was based on preliminary nonlinear time–history analyses conducted on a finite element model of the prototype structure used to assess the performance of the mock-up to be tested in the laboratory, as described in Section 4.

4. Numerical model and simulations

A 2D model of the building, illustrated in Fig. 10 was created in OpenSees. Opensees was used because it is suitable for multi-hazard analysis such as FFE analysis [43]. In this paper, only the numerical analyses relevant to the experimental tests performed at the JRC are presented. Thus, the results obtained by applying the ground motion presented in Section 3 were described. In this respect, nonlinear finite beam elements were used for all elements to check that non-dissipative elements remained in the elastic field under the seismic action. In particular, seven nonlinear fibre-based beam elements based on corotational formulation and the uniaxial Giuffre–Menegotto–Pinto steel material, with isotropic strain hardening (Steel02Material/SteelFFEThermal) [7,40] were used for each of the 4 members composing the concentric bracing system [44]. It is worth pointing out that the yield strength of the bracings was taken as the expected value, i.e. 330 MPa, considering a coefficient of variation equal to 0.12. In order to be also suitable for thermomechanical analysis, the columns were discretized with 15 elements considered continuous along the height of the structure and all connections of the beams and diagonals were assumed as pinned. Both global and member imperfections were included in the model and their magnitude was selected in accordance with EN 1993-1-1 [45]. Masses were considered lumped at the floors, following the assumption of rigid diaphragms.

Fig. 11 illustrates the results of the numerical simulation of the seismic test on the bare structure, i.e. without fire protections and firewalls, for the selected acceleration time–history. Fig. 11a shows the final deformed configuration of the steel frame at the end of the simulation. The horizontal displacements of each floor are shown in Fig. 11b, and the axial forces of the columns at the ground floor are depicted in Fig. 11c. As is possible to observe in Fig. 11d, the energy dissipation is concentrated in the braces and, in particular, at the ground floor. The internal columns and all the other elements remained in the elastic field during the seismic event. Moreover, the horizontal displacement of the 1st floor was within the limit ±30 mm range.

5. Experimental campaign

Large-scale tests of an entire structure are generally prohibitively expensive in terms of costs and time because of the need for expensive specialized facilities. As a result, hybrid simulation emerged as a viable solution for performing component-level experiments that account for the interaction between the tested specimen and a realistic yet virtual sub-assembly instantiated in a finite element software. For instance, large-scale tests with hybrid simulation techniques in the seismic field were successfully performed on a concrete bridge by Abbiati et al. [31] and on steel frames by Andreotti et al. [32,33]. Memari et al. [34] carried out a hybrid simulation test on a small-scale steel braced frame under fire and FFE. Moreover, Abbiati et al. developed partitioned algorithms both for seismic [46] and fire [47] applications. In the hybrid simulation context, the experimental full-scale mock-up, representative of only the ground floor of the prototype four-storey structure, was built at the ELSA Laboratory of the JRC, as illustrated in Fig. 12. As

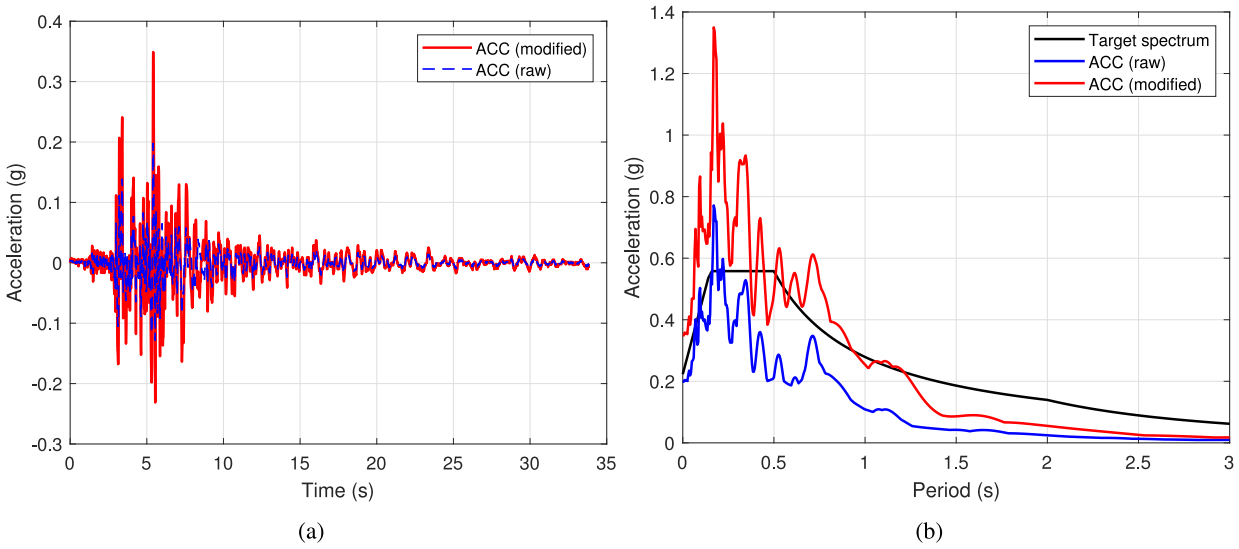

Fig. 9. (a) Original and modified N-S ground acceleration time–history of Patras earthquake (1994); (b) Patras N-S ground accelerogram compared to EC8 response spectrum.

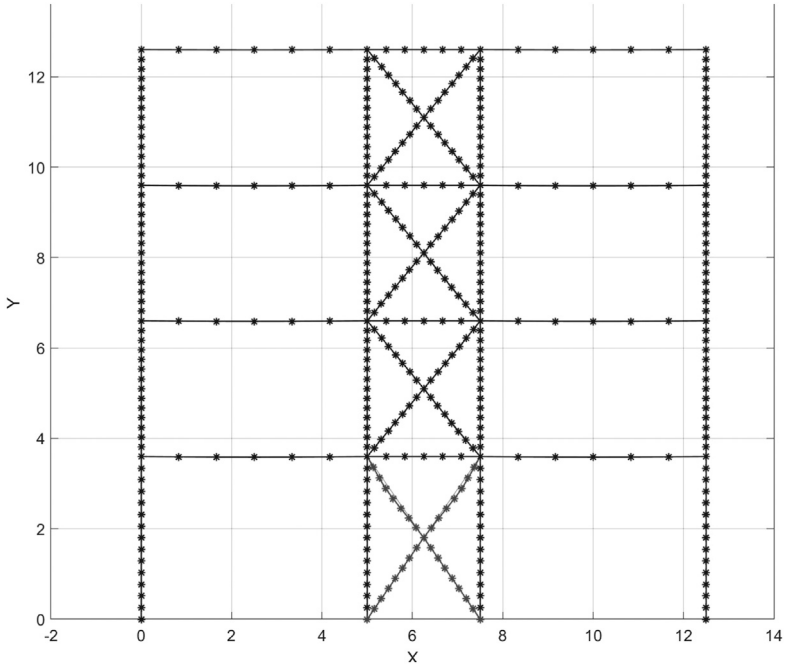

Fig. 10. Finite element discretization of the 2D numerical model of the frame.

can be observed in Fig. 14, only three degrees of freedom (DOFs) are coupled between the physical and numerical substructures. In fact, a master–slave relation is imposed on all horizontal DOFs of the first storey to follow DOF (DOF 1). Since external columns are connected to the braced frame by means of truss elements, the vertical displacement at their base was blocked on the numerical substructure. In order to enable hybrid simulation with mixed force- and displacement-controlled degrees of freedom (DOFs), a specific simulation algorithm was developed. Indeed, for each test, the horizontal actuator operated in displacement control, while the vertical actuators operated in force control. For the sake of simplicity and space, the full description of the algorithm will be described in a future work.

On these premises, the three-bay steel frame with concentric bracing in the central bay was assembled and a secondary frame, parallel to the main one, was used to stabilize the specimen for any possible out-of-plane instability during the test. The two frames were fixed to the strong floor and tare-connected together by steel rods, which did not alter the seismic response of the mock-up. Two 600 kN hydraulic actuators applied the vertical load on each column composing the bracing system, whereas lateral loads were applied through 500 kN

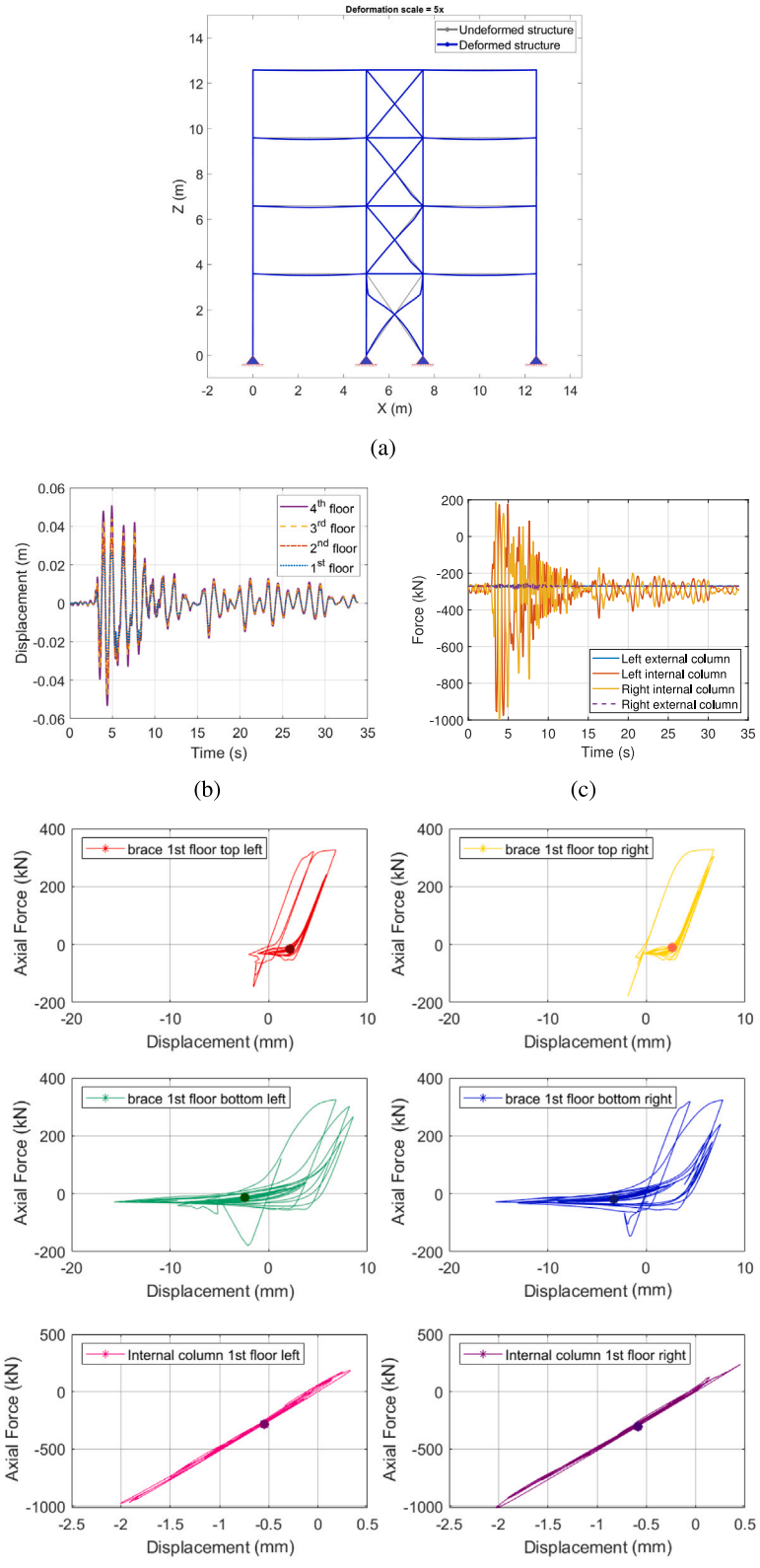

Fig. 11. (a) Deformed shape of the numerical model at the end of the simulation; (b) horizontal displacements of each floor; (c) axial force; (d) Axial force versus axial displacement response.

(a) (b)

Fig. 12. (a) General view of the specimen and experimental setup at the ELSA Reaction Wall; (b) detail of the bracing system.

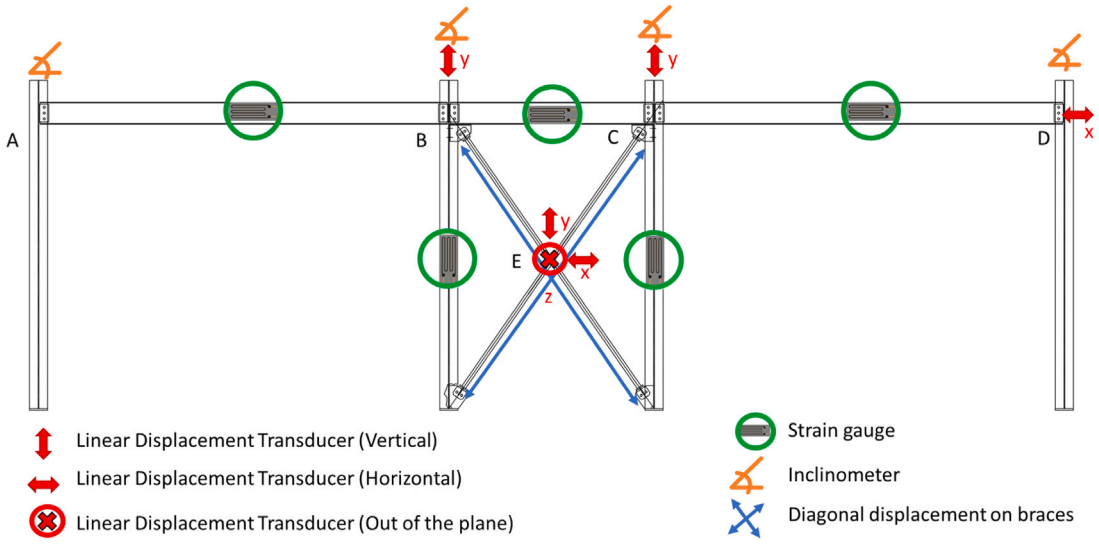

Fig. 13. Sensors location.

actuators connected to the reaction wall, one for the main frame and another for the secondary frame.

Load cells measured the loads applied by the vertical and horizontal actuators. Since the frame is statically indeterminate, the two central columns and the three beams were equipped with strain gauges that measured their internal axial strain. Displacement transducers measured the vertical deformation of the central columns, the axial strain of the braces, as well as the lateral displacement of the whole frame. Fig. 13 shows the sensor location.

To further reduce any possible interference from the secondary frame and eliminate any relative displacement during testing, the actuator of the secondary frame applied the same displacement as the horizontal actuator applied to the main frame.

5.1. Experimental programme

The experimental programme consisted of a series of hybrid simulation and cyclic tests performed on 4 different specimens:

- Frame A, bare frame without fire protection;
- Frame B, frame equipped with fire protection boards not designed for seismic regions;
- Frame C, frame equipped with fire protection boards designed for seismic regions;
- Frame D, frame equipped with sprayed-based fire protection, designed for seismic regions, and with two firewalls built in the external bays. The two firewalls were installed in such a way that the concrete blocks were not in direct contact with the steel frame, leaving a gap of 12 mm that was filled with material to guarantee the fire resistance requirement, as shown in Fig. 8.

Two hybrid simulation tests were carried out for each frame, as reported in Table 4. The scope of the second hybrid simulation test was to simulate a large aftershock test by remaining close to the ±30 mm range of horizontal displacement. Since the horizontal displacement was below this range for tests C-EQ1 and C-EQ2, a further cyclic test

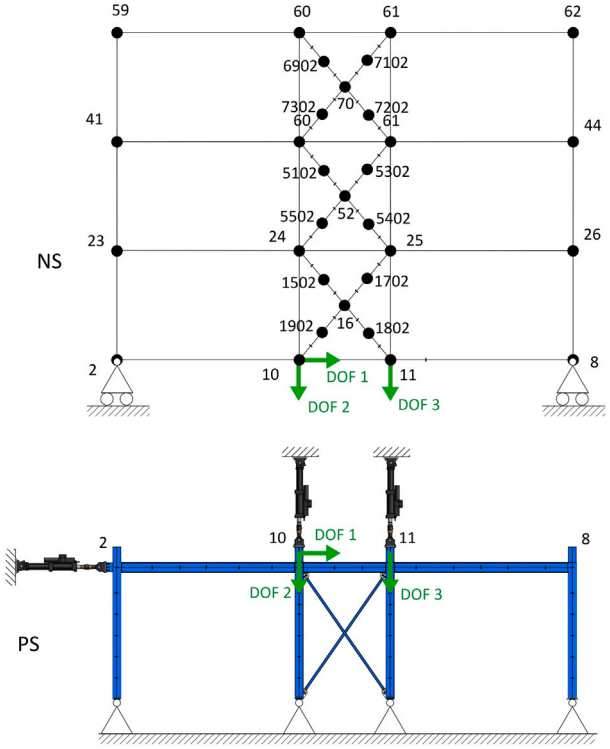

Fig. 14. Substructuring scheme adopted for the hybrid simulation tests.

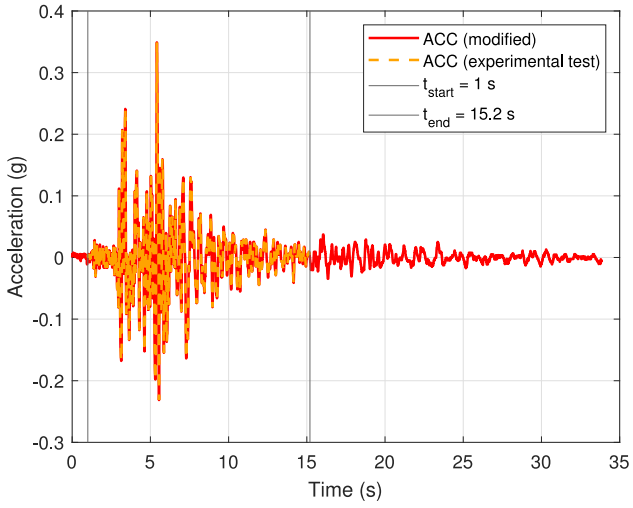

Fig. 15. Earthquake acceleration time–history.

C–CYC of amplitude ±30 mm was performed on Frame C. For the same reason, a final cyclic "funeral test" (D-CYC) was performed on Frame D comprising the firewalls. The maximum horizontal displacement for test D-CYC was ±35 mm, because it was hard to see damage in the walls at ±30 mm. As explained in Section 3, among the fifteen accelerograms, the one shown in Fig. 15 was selected. However, only the most significant portion of the full accelerogram (see Fig. 15) was used for the experimental hybrid simulation tests to reduce the total time of each test.

6. Experimental tests

The results of the experimental tests are hereinafter described.

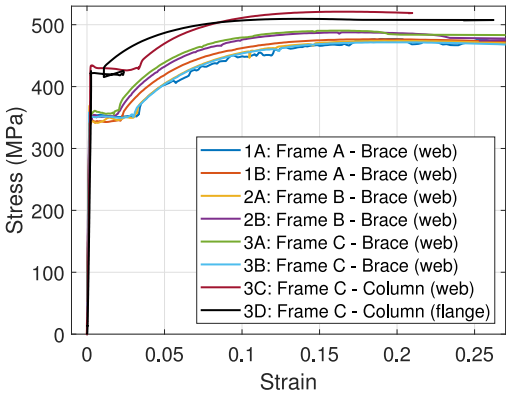

Fig. 16. Material coupon tests.

Table 4
Experimental programme.

Test ID	JRC ID	Test type	Fire protection
A - EQ1	A-32	Mainshock	None
A - EQ2	A-33	Aftershock	None
B - EQ1	B-06	Mainshock	Standard fire protection boards
B - EQ2	B-07	Aftershock	Standard fire protection boards
C - EQ1	C-04	Mainshock	Reinforced fire protection boards
C - EQ2	C-05	Aftershock	Reinforced fire protection boards
C - CYC	C-06	Cyclic	Reinforced fire protection boards
D - EQ1	D-03	Mainshock	Reinforced spray-based fire protection and firewalls
D - EQ2	D-04	Aftershock	Reinforced spray-based fire protection and firewalls
D - CYC	D-05	Cyclic	Reinforced spray-based fire protection and firewalls

Table 5
Material properties of structural steel.

Label	Tested component	Steel grade	Yield strength (MPa)	Ultimate tensile strength (MPa)
1A	Brace (web)	S275	345.5	466.6
1B	Brace (web)	S275	343.4	474.4
2A	Brace (web)	S275	368.0	471.6
2B	Brace (web)	S275	351.1	485.0
3A	Brace (web)	S275	359.3	488.3
3B	Brace (web)	S275	355.8	469.6
3C	Column (web)	S355	431.9	518.3
3D	Column (flange)	S355	425.1	508.7

6.1. Material properties

Material tests were performed on the structural steel. As previously mentioned, the columns and beams were made of S355 steel, while the braces were made of S275 steel. Several material coupons were extracted from the specimens: from the flanges and the web, parallel to the rolling direction. As a result, the stress–strain relationships are reported in Fig. 16, and the data are reported in Table 5.

6.2. Test results

6.2.1. Hybrid simulations

Figs. 17 and 18 present the horizontal force–displacement curves, vertical forces and vertical displacements of the first and second hybrid simulation tests for each frame, respectively. The results in terms of maximum displacement and force are reported in Table 6. From Fig. 17, it is possible to observe that the bare frame (Frame A) and the specimens with the fire protection boards with (Frame B) and without (Frame C) seismic design showed similar responses. Frame B practically

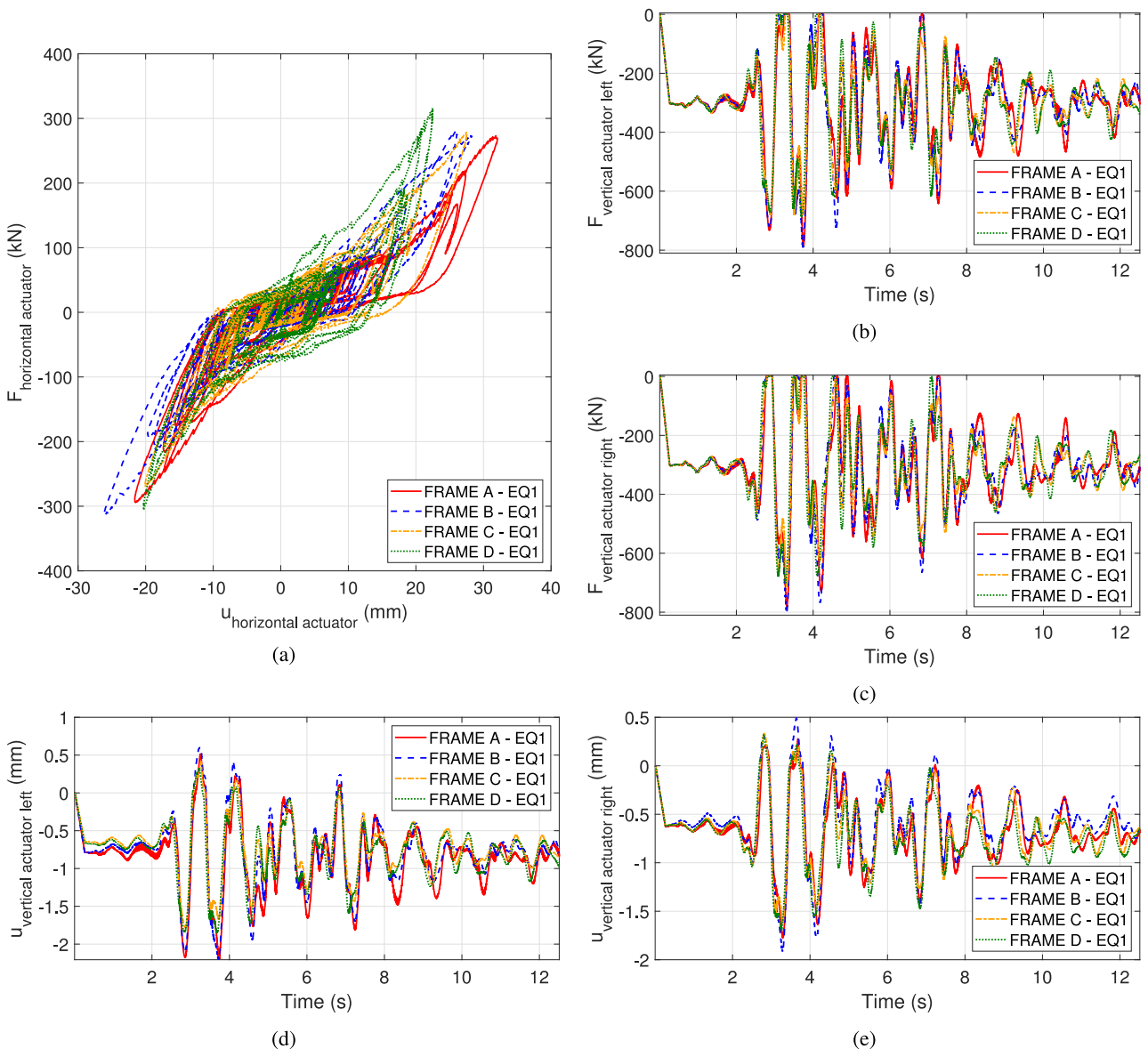

Fig. 17. Results of the 1st hybrid simulation tests (Mainshock): (a) force–displacement curves; (b) vertical displacement of the left actuator (DOF 2); (c) vertical displacement of the right actuator (DOF 3).

exhibited the same displacement (+1%), while Frame C showed a moderate reduction (−11%). Compared with panels directly attached to the frame, the metal profiles used to fasten the protection boards in Frame B probably introduce a mechanical decoupling between the frame and the panels. On the other hand, this feature preserves boards against seismic deformations transferred by the frame. Frame B and C dissipated more energy than the Frame A, i.e. +14% and +23% respectively (see Table 6). This could be attributed to the metallic substructure of the fire protection boards with seismic design. As expected, Frame D with sprayed-based fire protection and the firewalls showed smaller displacement, i.e. −20%, which means, on average, higher stiffness and higher resistance than the other configurations, i.e. +8%, along with higher dissipated energy (+32%). In fact, once the displacement was approximately 12 mm, the firewalls directly interacted with the steel frame. Moreover, it is interesting to note that when the vertical displacement became positive (see Fig. 17d and e), i.e. the columns were in tension, the partitioned algorithm put the force of the vertical actuators to zero.

Similar behaviour was observed when the frames were subjected to the second hybrid simulation test, i.e. the aftershock, as illustrated in Fig. 18. Despite the frames being partly damaged by the first hybrid simulation test, no appreciable differences in the overall seismic response could be detected. Only Frame D lost some of its dissipation capability (−12%) with respect to the main shock.

6.2.2. *Cyclic tests*

The time histories of the horizontal displacement and the vertical forces imposed on the frame are illustrated respectively in Fig. 19a and b. The horizontal displacement imposed on the frame consisted of:

- three cycles at ±30 mm for Frame C.
- three cycles at ±30 mm and two cycles at ±35 mm for Frame D.

The vertical forces imposed on the frame consisted of:

- three cycles from 0 to −600 kN or Frame C.
- five cycles from 0 to −600 kN or Frame D.

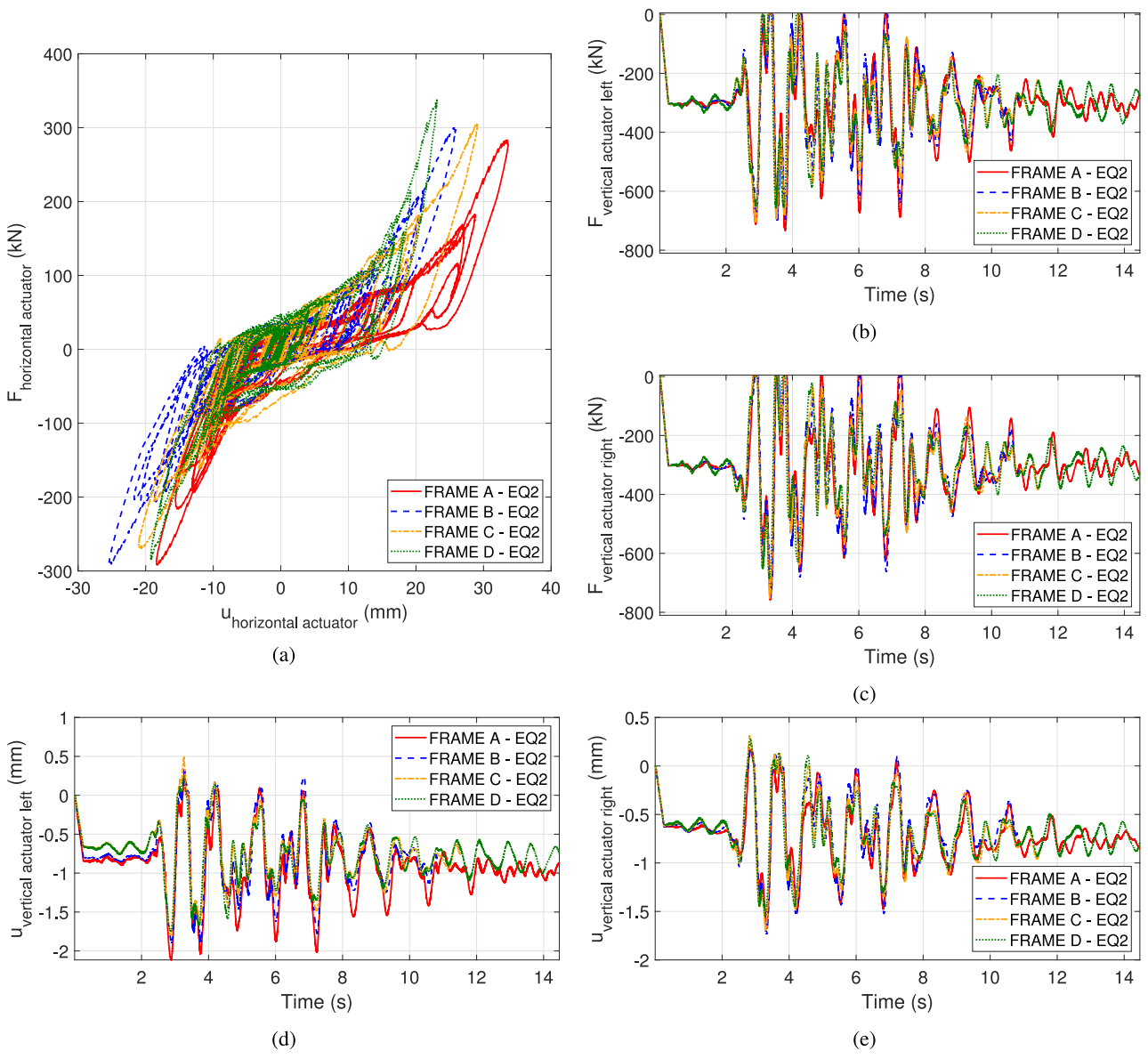

Fig. 18. Results of the 2nd hybrid simulation tests (Afteshock): (a) force–displacement curves; (b) vertical displacement of the left actuator (DOF 2); (c) vertical displacement of the right actuator (DOF 3).

Table 6
Seismic tests results.

Seismic response compared to the bare frame (A) in the first shock										
EQ1	Displacement (mm)				Force (kN)				Energy (kJ)	
	d_{max}	d_{min}	Δd	$\Delta d_{i/A}$	F_{max}	F_{min}	ΔF	$\Delta F_{i/A}$	E	$\Delta E_{i/A}$
Frame A	32.03	−21.63	53.66	–	268.5	−288.4	557.0	–	12.58	–
Frame B	28.20	−26.11	54.31	+1%	271.5	−310.4	581.9	+4%	14.36	+14%
Frame C	27.52	−20.09	47.61	−11%	274.2	−265.1	539.4	−3%	15.51	+23%
Frame D	22.46	−20.31	42.77	−20%	302.1	−297.7	599.9	+8%	16.56	+32%
Comparison between first shock and aftershock										
EQ2	Displacement (mm)				Force (kN)				Energy (kJ)	
	d_{max}	d_{min}	Δd	$\Delta d_{EQ2/EQ1}$	F_{max}	F_{min}	ΔF	$\Delta F_{EQ2/EQ1}$	E	$\Delta E_{EQ2/EQ1}$
Frame A	33.60	−18.42	52.02	−3%	278.5	−286.0	564.5	+1%	12.06	−4%
Frame B	25.82	−25.42	51.24	−6%	297.2	−289.6	586.8	+1%	13.66	−5%
Frame C	29.04	−21.03	50.07	+5%	302.3	−264.3	566.6	+5%	14.97	−3%
Frame D	23.07	−19.23	42.29	−1%	336.9	−276.9	613.8	+2%	14.53	−12%

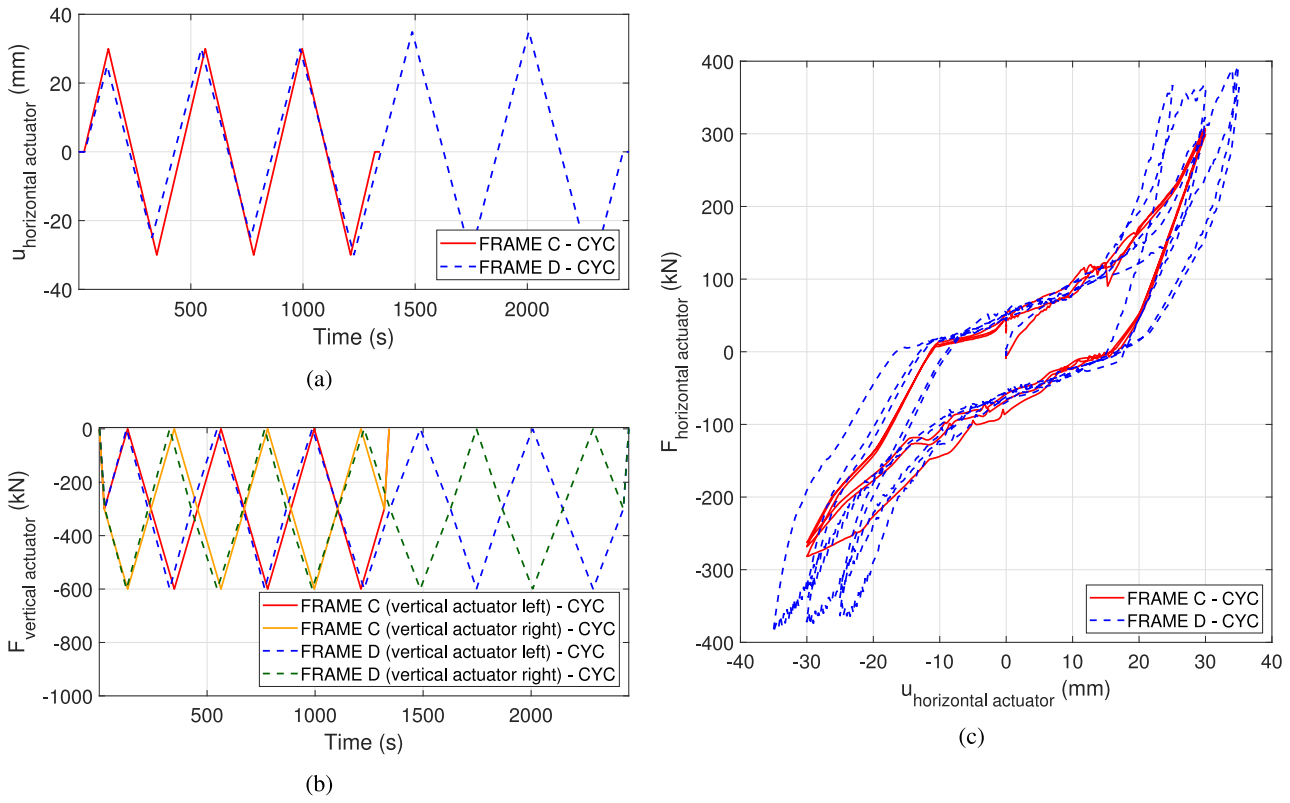

Fig. 19. Cyclic tests: (a) horizontal displacement imposed time–history (DOF 1); (b) vertical forces imposed time–history (DOF 2 and DOF 3); (c) force–displacement curves.

Table 7
Cyclic tests results.

	CYC			
	Displacement (mm)		Force (kN)	
	+	−	+	−
Frame C	30	30	300	269
Frame D	35	35	395	375

As previously mentioned, the cyclic tests were intended to induce more damage to Frame C and D, while keeping the maximum horizontal displacement within 30 mm (inter-storey drift ratio 0.8%) and 35 mm (inter-storey drift ratio 1.0%), respectively. Fig. 19c presents the resulting force–displacement curves for the cyclic tests. It may be noted that for Frame C, despite an increase in horizontal displacement, the maximum measured horizontal force when pulling back the frame (negative sign) is essentially the same as for the second hybrid simulation test, as shown in Fig. 18a. Indeed, from the figure, it is possible to observe a change of stiffness owing to the buckling of one of the braces in compression, as illustrated in Fig. 22. This phenomenon is less evident in Frame D; however, the stiffness variation is still observable in the last cycle when the frame was pulled back (negative sign) because of the buckling of one of the braces in compression, as depicted in Fig. 23. The results are reported in Table 7.

6.2.3. Damages

No significant damage was observed after the test on the bare frame, i.e. Frame A. In fact, buckling of the braces was not observable. During the hybrid simulation tests on Frame B and C, small cracks were observed on the fire protection boards applied to the braces, as shown in Figs. 20 and 21, whereas, as expected, no damage was detected on the columns as they are non-dissipative members. Nevertheless, the extent of damage to the fire protections is not expected to affect their fire performance. Indeed, despite the accelerogram being modified to be compatible with the elastic spectrum at the life safety limit state, the maximum inter-storey drift was equal to 0.8%, which corresponds to moderate yielding and buckling of the braces according to the FEMA-356 [41]. Tests were then carried out with repeated cycles of frames C and D, which induced buckling of the braces, along with some damage to the fire protection elements applied to the braces, as illustrated in Fig. 22. It is worth pointing out that in Fig. 22 the boards were removed after the test in order to better identify the damage to the brace; thus, the boards did not fall off from the brace during the test, and only some cracks were detected, as shown in Fig. 22. Analogously, Frame D with spray-based fire protection and firewalls did not exhibit significant damage during the D-EQ1 and D-EQ2 hybrid simulation tests. Conversely, during the D-CYC cyclic test, the braces buckled and a diagonal crack passing through the masonry blocks and the mortar joints developed at the lower corner of the wall without seismic design, and the firewalls were detached from the columns and the floor, as shown in Fig. 23. In contrast, the firewall reinforced against the seismic action did not exhibit appreciable damage. In sum, the most visible damage after tests C–CYC and D-CYC (Figs. 22 and 23) was on the braces because of buckling. Again, the extent of damage to fire protections was not expected to affect the fire performance significantly. Before and after each test, several photos of the frame were taken to reconstruct a 3D model of the frame using photogrammetry. Photogrammetry allows visual comparisons and measurements to evaluate the damage evolution before and after each test. For example, Fig. 24, illustrates the 3D reconstruction of Frame D before and after the tests.

7. Conclusive remarks

The paper presented the results of an experimental analysis of the seismic behaviour of a concentrically braced steel frame with the aim

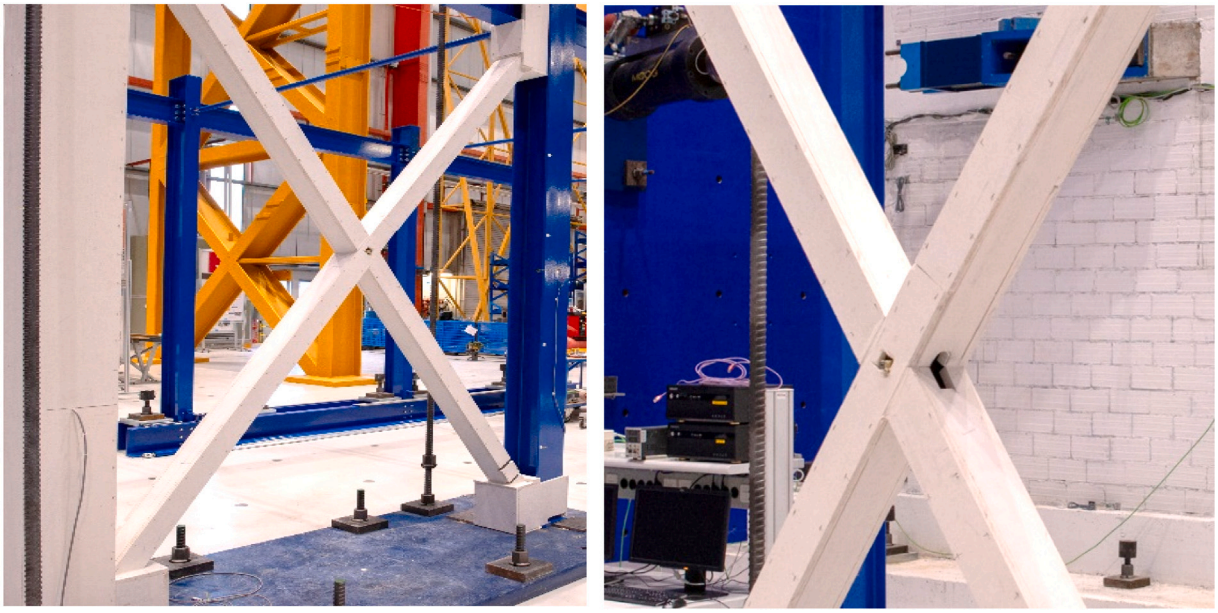

Fig. 20. Damage state of Frame B after test B-EQ2: (a) bracing system; (b) enlargement of the brace crossing.

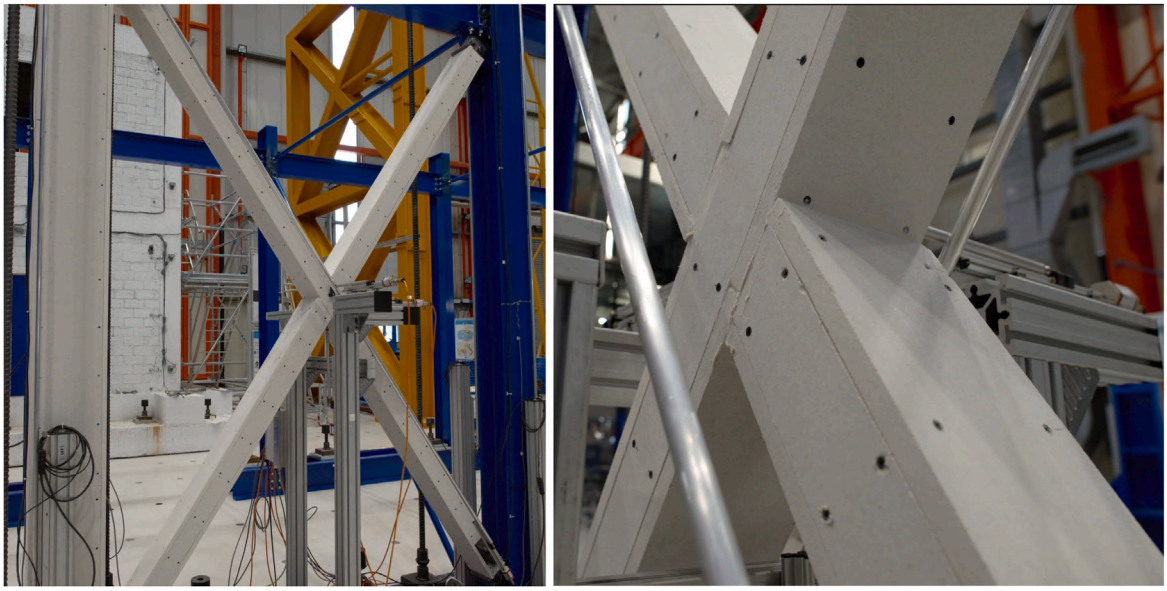

Fig. 21. Damage state of Frame C after test B-EQ2: (a) bracing system; (b) enlargement of the brace crossing.

to study the performance of structural and non-structural components. A total of ten seismic tests were performed at the ELSA Reaction Wall of the JRC. In particular, full-scale seismic testing by means of hybrid simulation was successfully performed. The tests allowed to investigate the seismic response of different types of fire protection elements: calcium silicate boards with and without seismic design, spray-based fire protection, firewalls with and without seismic design and their interaction with the structural elements. Moreover, it was possible to analyse the variations in seismic response induced by non-structural elements (fire protections and firewalls) subjected to a sequence of two identical shocks (first shock and aftershock). Hybrid simulation tests showed that frames with fire protections and firewalls had higher dissipation capacity than the bare frame. The frame equipped with seismic reinforced calcium silicate boards dissipated more energy than the bare frame (+23%) and than the frame with standard calcium silicate boards (+8%). Moreover, the frame with the firewalls exhibited lower horizontal displacements, i.e. −20%, with respect to the bare frame due to the higher stiffness. A maximum inter-storey drift ratio of 0.8%, during the hybrid simulation tests, and 1.0% for the cyclic tests were recorded. The aftershock hybrid simulation tests showed similar results with respect to the main shock. Only the frame equipped with the firewalls lost some of its dissipation capacity (−12%) with respect

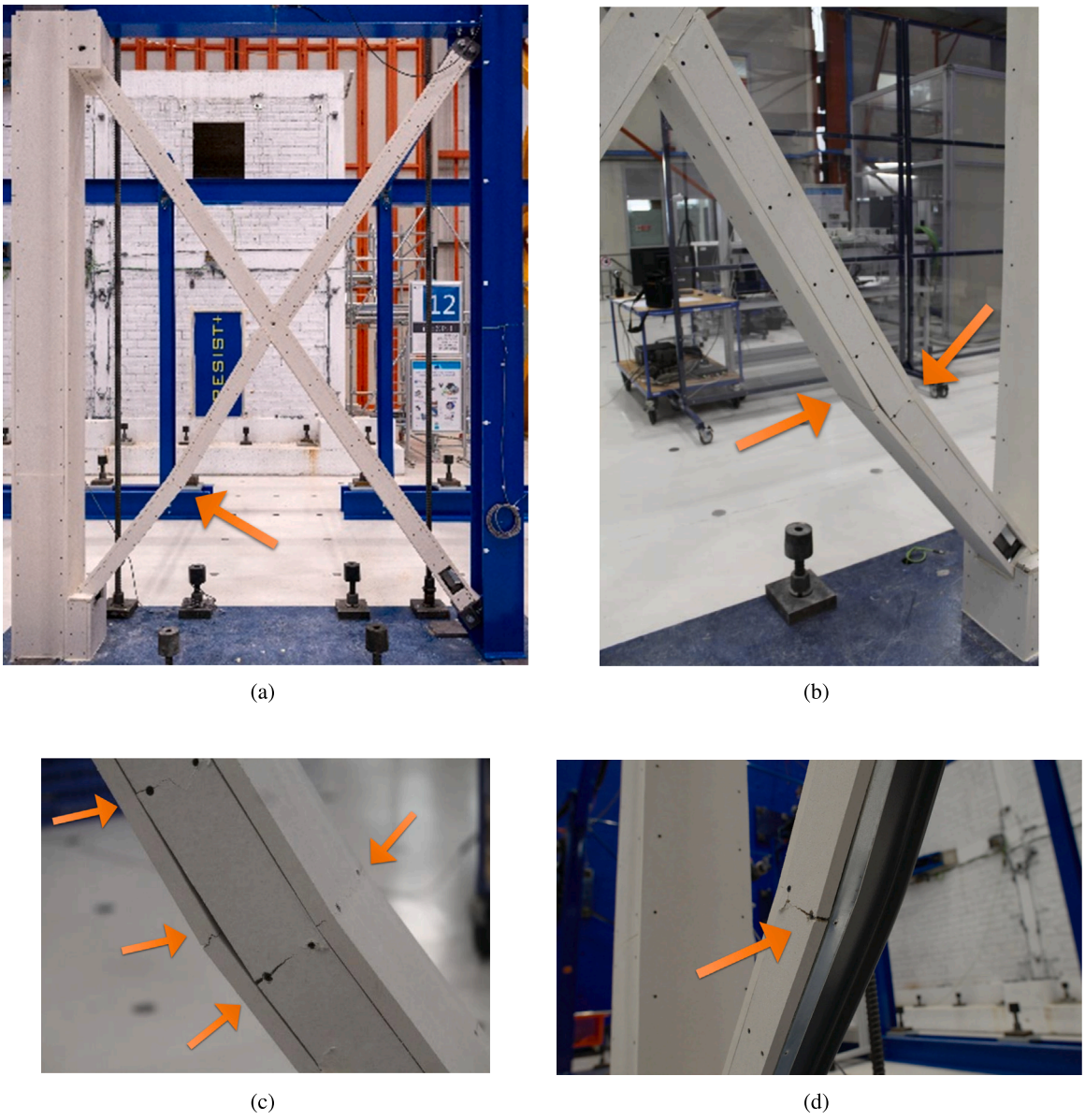

Fig. 22. Damage state of Frame C after test C–CYC: (a) bracing system; (b) buckled brace; (c–d) enlargement of the buckled brace.

to the main shock. Tests conducted with a larger number of cycles at maximum amplitude caused buckling of the braces and damage to the fire protection elements. In fact, some cracks in the fire protections applied to the braces were observed (both boards and spray-based) and in the firewall without seismic design. Nevertheless, because of the inter-storey drift values, the damage level of the fire protections was not expected to affect the fire performance significantly. In addition, even at low drift values, the change in the seismic response of the system induced by the fire protection could be observed and quantified. In order to extend the experimental results obtained in this study to structures with higher inter-storey drift values, further experimental campaigns should focus on more flexible structures, such as moment-resisting frames. The results indicate that compliance with the standard design limit states, which restrict the maximum displacement, is in itself an effective method for the prevention of seismic damage to fire protection systems.

CRediT authorship contribution statement

Patrick Covi: Data curation, Formal analysis, Investigation, Methodology, Software, Validation, Visualization, Writing – original draft, Writing – review & editing. **Nicola Tondini:** Conceptualization, Data curation, Investigation, Methodology, Supervision, Writing – original draft, Writing – review & editing. **Marco Lamperti Tornaghi:** Data curation, Investigation, Methodology, Supervision, Writing – original draft, Writing – review & editing. **Francisco-Javier Molina:** Investigation, Methodology, Resources. **Pierre Pegon:** Investigation, Methodology, Resources, Software. **Georgios Tsionis:** Funding acquisition, Project administration.

(a)

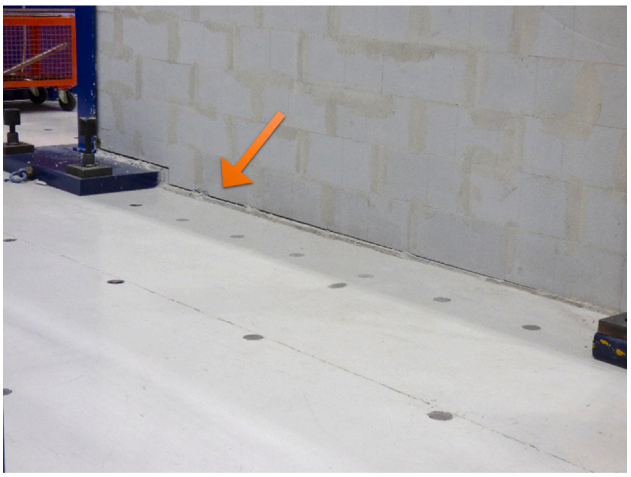

(b)

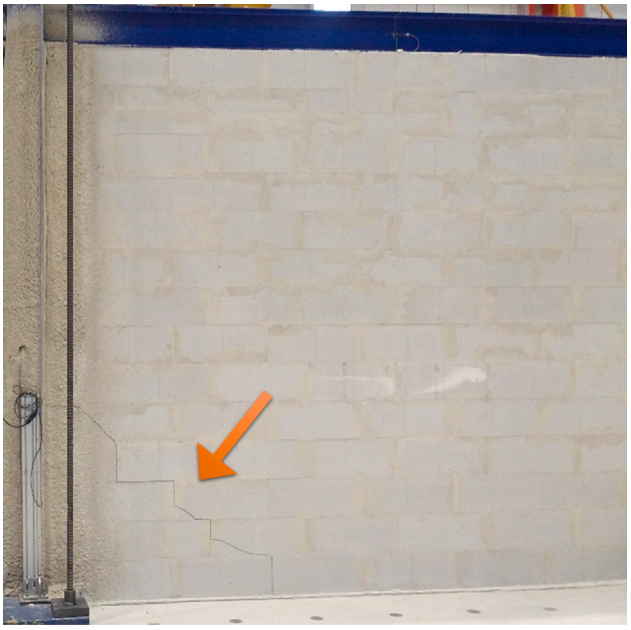

(c)

Fig. 23. Damage state of Frame D after test D-CYC: (a) bracing system; (b) base of the firewall; (c) cracks on the firewall without seismic design.

Declaration of competing interest

The authors declare that they have no known competing financial interests or personal relationships that could have appeared to influence the work reported in this paper.

Data availability

Data will be made available on request.

Acknowledgements

This work has received funding from the European Union's Horizon 2020 research and innovation program under the SERA grant agreement No. 730900 and the related TA project EQUFIRE. The first and the second authors acknowledge the Italian Ministry of Education, Universities and Research (MUR) in the framework of the project DICAM-EXC (Departments of Excellence 2023–2027 grant L 232/2016). Marco Antonelli (Promat) and Alessandro Miliani (Xella) are gratefully acknowledged for their technical support.

The EQUFIRE project aimed at providing sound experimental evidence and data on the performance of structural and non-structural components, and their interaction with different conventional and seismic-resistant fire protection systems, of steel frames subjected to scenarios of fire following earthquake. EQUFIRE was selected for Transnational Access to the ELSA Reaction Wall of the European Commission's Joint Research Centre, within the Horizon 2020 SERA project (2017–2020, www.sera-eu.org) The EQUFIRE team of users comprised 11 researchers from the Federal Institute for Materials Research and Testing (DE), University of Trento (IT), Aarhus University (DK), Swiss Seismological Service (CH), Promat SpA (IT) and Xella Italia Srl (IT). The experimental programme included seismic tests of a real-scale one-storey frame at the ELSA Reaction Wall and tests of columns subjected to fire following earthquake at the Bundesanstalt für Materialforschung und -prüfung (BAM) (Federal Institute for Materials Research and Testing).

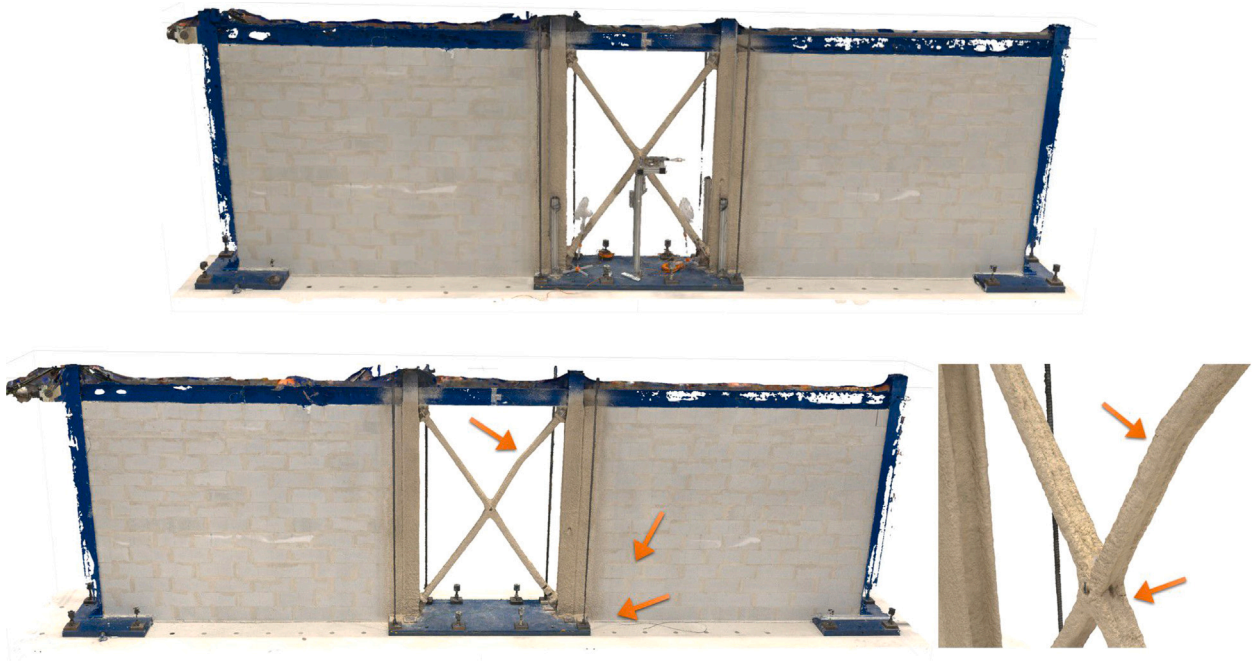

Fig. 24. 3D model of Frame D obtained using the photogrammetry methodology: (a) before the tests; (b) after the cyclic tests.

References

[1] Scawthorn Charles, Eidinger John M, Schiff Anshel. Fire following earthquake, Vol. 26. ASCE Publications; 2005.

[2] Elhami Khorasani Negar, Garlock Maria EM. Overview of fire following earthquake: Historical events and community responses. International Journal of Disaster Resilience in the Built Environment 2017;8(02):158–74.

[3] Botting Russ. The impact of post-earthquake fire on the built urban environment: A report submitted in partial fulfilment of the requirements for the degree of master of engineering in fire engineering at the University of Canterbury, Christchurch, New Zealand (Ph.D. thesis), University of Canterbury; 1998.

[4] Himoto Keisuke. Comparative analysis of post-earthquake fires in Japan from 1995 to 2017. Fire Technology 2019;55(3):935–61.

[5] Sarreshtehdari Amir, Elhami Khorasani Negar. Post-earthquake emergency response time to locations of fire ignition. Journal of Earthquake Engineering 2022;26(7):3389–416.

[6] Coar Maxwell, Sarreshtehdari Amir, Garlock Maria, Elhami Khorasani Negar. Methodology and challenges of fire following earthquake analysis: an urban community study considering water and transportation networks. Natural Hazards 2021;109(1):1–31.

[7] Covi Patrick, Tondini Nicola, Sarreshtehdari Amir, Elhami-Khorasani Negar. Development of a novel fire following earthquake probabilistic framework applied to a steel braced frame. Structural Safety 2023;105:102377.

[8] Taylor John. Post earthquake fire in tall buildings and the New Zealand building code. University of Canterbury; 2003.

[9] Possidente Luca, Tondini Nicola. Validation of a new analytical formula to predict the steel temperature of heavily insulated cross-sections. Fire Technology 2023;1–23. http://dx.doi.org/10.1007/s10694-023-01511-7.

[10] Possidente Luca, Tondini Nicola, Wickström Ulf. Derivation of a new temperature calculation formulation for heavily fire insulated steel cross-sections. Fire Safety Journal 2023;141:103991. http://dx.doi.org/10.1016/j.firesaf.2023.103991.

[11] Sajid Hizb Ullah, Kiran Ravi. Post-fire mechanical behavior of ASTM A572 steels subjected to high stress triaxialities. Engineering Structures 2019;191:323–42.

[12] Braxtan Nicole Leo, Pessiki Stephen P. Postearthquake fire performance of sprayed fire-resistive material on steel moment frames. Journal of Structural Engineering 2011;137(9):946–53.

[13] Keller Wesley J, Pessiki Stephen. Effect of earthquake-induced damage to spray-applied fire-resistive insulation on the response of steel moment-frame beam-column connections during fire exposure. Journal of Fire Protection Engineering 2012;22(4):271–99.

[14] Pucinotti Raffaele, Bursi OS, Demonceau Jean-François. Post-earthquake fire and seismic performance of welded steel–concrete composite beam-to-column joints. Journal of Constructional Steel Research 2011;67(9):1358–75.

[15] Pucinotti Raffaele, Bursi OS, Franssen Jean-Marc, Lennon Tom. Seismic-induced fire resistance of composite welded beam-to-column joints with concrete-filled tubes. Fire Safety Journal 2011;46(6):335–47.

[16] Ye Zhongnan, Jiang Shouchao, Heidarpour Amin, Li Yingchao, Li Guoqiang. Experimental study on cyclically-damaged steel-concrete composite joints subjected to fire. Steel and Composite Structures 2019;30(4):351–64.

[17] Song Qian-Yi, Heidarpour Amin, Zhao Xiao-Ling, Han Lin-Hai. Post-earthquake fire behavior of welded steel I-beam to hollow column connections: An experimental investigation. Thin-Walled Structures 2016;98:143–53.

[18] Imani Reza, Mosqueda Gilberto, Bruneau M. Experimental study on post-earthquake fire resistance of ductile concrete-filled double-skin tube columns. Journal of Structural Engineering 2015;141(8):04014192.

[19] Wang JH, Kunnath S, He J, Xiao Y. Post-earthquake fire resistance of circular concrete-filled steel tubular columns. Journal of Structural Engineering 2020;146(6):04020105.

[20] Lou Ting, Wang Wei, Li Junlin. Post-earthquake fire behaviour of a self-centring connection with buckling-restrained plates and pre-stressed bars: An experimental investigation. Journal of Building Engineering 2022;56:104733.

[21] Kamath Praveen, Sharma Umesh Kumar, Kumar Virendra, Bhargava Pradeep, Usmani Asif, Singh Bhupinder, Singh Yogendra, Torero Jose, Gillie Martin, Pankaj Pankaj. Full-scale fire test on an earthquake-damaged reinforced concrete frame. Fire Safety Journal 2015;73:1–19.

[22] Meacham Brian J. Post-earthquake fire performance of buildings: Summary of a large-scale experiment and conceptual framework for integrated performance-based seismic and fire design. Fire Technology 2016;52(4):1133–57.

[23] Pantoli Elide, Chen Michelle C, Wang Xiang, Astroza Rodrigo, Ebrahimian Hamed, Hutchinson Tara C, Conte Joel P, Restrepo José I, Marin Claudia, Walsh Kenneth D, et al. Full-scale structural and nonstructural building system performance during earthquakes: Part II–NCS damage states. Earthquake Spectra 2016;32(2):771–94.

[24] Shah Asif H, Sharma Umesh Kumar, Bhargava Pradeep. Outcomes of a major research on full scale testing of RC frames in post earthquake fire. Construction and Building Materials 2017;155:1224–41.

[25] Hutchinson Tara C, Wang Xiang, Hegemier Gilbert, Kamath Praveen, Meacham Brian. Earthquake and postearthquake fire testing of a midrise cold-formed steel-framed building. I: Building response and physical damage. Journal of Structural Engineering 2021;147(9):04021125.

[26] Calayir Muhammet, Selamet Serdar, Wang Yong C. Post-earthquake fire performance of fire door sets. Fire Safety Journal 2022;130:103589.

[27] Tian Yuan, Filiatrault Andre, Mosqueda Gilberto. Seismic response of pressurized fire sprinkler piping systems I: experimental study. Journal of Earthquake Engineering 2015;19(4):649–73.

[28] FEMA P. 58. Next-generation methodology for seismic performance assessment of buildings. Appl Technol Council Federal Emerg Manage Agency 2012;2.

[29] Donea J, Magonette G, Negro P, Pegon P, Pinto A, Verzeletti G. Pseudodynamic capabilities of the ELSA laboratory for earthquake testing of large structures. Earthquake Spectra 1996;12(1):163–80.

[30] Pinto AV, Pegon Pierre, Magonette Georges, Tsionis Georgios. Pseudo-dynamic testing of bridges using non-linear substructuring. Earthquake engineering & structural dynamics 2004;33(11):1125–46.

[31] Abbiati Giuseppe, Bursi Oreste S, Caperan Philippe, Di Sarno Luigi, Molina Francisco Javier, Paolacci Fabrizio, Pegon Pierre. Hybrid simulation of a multi-span RC viaduct with plain bars and sliding bearings. Earthquake Engineering & Structural Dynamics 2015;44(13):2221–40. http://dx.doi.org/10.1002/eqe.2580, URL http://doi.wiley.com/10.1002/eqe.2580.

[32] Andreotti Roberto, Giuliani Giulia, Tondini Nicola. Experimental analysis of a full-scale steel frame with replaceable dissipative connections. Journal of Constructional Steel Research 2023;208:108036.

[33] Andreotti Roberto, Giuliani Giulia, Tondini Nicola, Bursi Oreste S. Hybrid simulation of a partial-strength steel–concrete composite moment-resisting frame endowed with hysteretic replaceable beam splices. Earthquake Engineering & Structural Dynamics 2023;52(1):51–70.

[34] Memari Mehrdad, Wang Xuguang, Mahmoud Hussam, Kwon Oh-Sung. Hybrid simulation of small-scale steel braced frame subjected to fire and fire following earthquake. Journal of Structural Engineering 2020;146(1):04019182.

[35] Covi Patrick, Tondini Nicola, Korzen Manfred, Tsionis Georgios. Numerical-experimental analysis of a braced steel frame subjected to fire following earthquake. In: Proceedings of 9th European conference on steel and composite structures. 1-3 September.

[36] CEN. Eurocode 1 - actions on structures - part 1-1: General actions - Densities, self-weight, imposed loads for buildings. European standard, European Union; 2004.

[37] CEN. Eurocode 1 - actions on structures - part 1-3: General actions - snow loads. European standard, European Union; 2004.

[38] CEN. Eurocode 8: Design of structures for earthquake resistance - part 1: General rules, seismic actions and rules for buildings. European standard, European Union; 2004.

[39] Silva Vitor, Crowley Helen, Varum Humberto, Pinho Rui. Seismic risk assessment for mainland Portugal. Bulletin of Earthquake Engineering 2015;13(2):429–57.

[40] McKenna Frank. OpenSees: a framework for earthquake engineering simulation. Computing in Science & Engineering 2011;13(4):58–66.

[41] FEMA. Prestandard and commentary for the seismic rehabilitation of buildings. Technical report, Federal Emergency Management Agency; 2000.

[42] Luzi Lucia, Puglia R, Russo E, Orfeus WG. Engineering strong motion database, version 1.0, Vol. 10. Istituto Nazionale di Geofisica e Vulcanologia, Observatories & Research Facilities for European Seismology; 2016, doi.

[43] Covi Patrick. Multi-hazard analysis of steel structures subjected to fire following earthquake (Ph.D. thesis), University of Trento; 2021, http://dx.doi.org/10.15168/11572_313383.

[44] Uriz Patxi, Filippou Filip C, Mahin Stephen A. Model for cyclic inelastic buckling of steel braces. Journal of Structural Engineering 2008;134(4):619–28.

[45] CEN. Eurocode 3: Design of steel structures - part 1-1: General rules and rules for buildings. European standard, European Union; 2005.

[46] Abbiati G, Lanese I, Cazzador E, Bursi O S, Pavese A. A computational framework for fast-time hybrid simulation based on partitioned time integration and state-space modeling. Structural Control and Health Monitoring 2019;26(e2419).

[47] Abbiati Giuseppe, Covi Patrick, Tondini Nicola, Bursi Oreste S, Stojadinović Božidar. A real-time hybrid fire simulation method based on dynamic relaxation and partitioned time integration. Journal of Engineering Mechanics 2020;146(9):04020104.